ACADEMIC PRESS

Available online at www.sciencedirect.com

SCIENCE DIRECT®

DEVELOPMENTAL BIOLOGY

Developmental Biology 255 (2003) 303–312

www.elsevier.com/locate/ydbio

The roles of *Pax6* in the cornea, retina, and olfactory epithelium of the developing mouse embryo

J. Martin Collinson,[a,*,1] Jane C. Quinn,[a,b] Robert E. Hill,[c] and John D. West[a]

[a] *Division of Reproductive and Developmental Sciences, Genes and Development Group, University of Edinburgh, Hugh Robson Building, George Square, Edinburgh EH8 9XD, Scotland, UK*

[b] *Division of Biomedical Sciences, Genes and Development Group, University of Edinburgh, Hugh Robson Building, George Square, Edinburgh EH8 9XD, Scotland, UK*

[c] *Comparative and Developmental Genetics Section, MRC Human Genetics Unit, Crewe Road, Edinburgh EH4 2XU, Scotland, UK*

Received for publication 14 August 2002, revised 5 November 2002, accepted 29 November 2002

Abstract

The roles of *Pax6* were investigated in the murine eye and the olfactory epithelium by analysing gene expression and distribution of $Pax6^{-/-}$ cells in $Pax6^{+/+} \leftrightarrow Pax6^{-/-}$ chimeras. It was found that between embryonic days E10.5 and E16.5 *Pax6* is autonomously required for cells to contribute fully not only to the corneal epithelium, where *Pax6* is expressed at high levels, but also to the to the corneal stroma and endothelium, where the protein is detected at very low levels. $Pax6^{-/-}$ cells contributed only poorly to the neural retina, forming small clumps of cells that were normally restricted to the ganglion cell layer at E16.5. $Pax6^{-/-}$ cells in the retinal pigment epithelium could express *Trp2*, a component of the pigmentation pathway, at E14.5 and a small number went on to differentiate and produce pigment at E16.5. The segregation and near-exclusion of mutant cells from the nasal epithelium mirrored the behaviour of mutant cells in other developmental contexts, particularly the lens, suggesting that common primary defects may be responsible for diverse *Pax6*-related phenotypes.

Keywords: Chimera; Chimaera; Pax6; Eye development; Olfactory epithelium; Cornea; Retina; Lens

Introduction

The transcription factor Pax6 is widely expressed throughout murine eye development in the lens, corneal epithelium, iris, ciliary body, all layers of the neural retina, and the retinal pigment epithelium (RPE) (Grindley et al., 1995; Hitchcock et al., 1996; Koroma et al., 1998; Walther and Gruss, 1991). At E9, *Pax6* is expressed in a broad domain of the facial epithelium, subsequently becoming restricted to the lens and nasal placodes at E10 (Grindley et al., 1995; Li et al., 1994). In mice that are homozygous null for *Pax6*, eye and olfactory system development stops at an early stage, with the failure of lens and nasal placode formation (Grindley et al., 1995; Hill et al., 1991; Hogan et al., 1986). This creates problems for the analysis of the roles of *Pax6* in tissues such as the corneal epithelium and retina (where the gene is normally expressed), which never form in the mutants, and does not allow analysis of later roles during the differentiation of the lens and olfactory epithelium.

Cre-*lox* tissue-specific knockouts of *Pax6* in the lens (Ashery-Padan et al., 2000) and the distal retina (Marquardt et al., 2001) have been used to address some of these issues. These studies showed that Pax6 is required for lens placode formation and that knocking out *Pax6* in neural retinal cells severely restricts their potential fates.

Previously (Collinson et al., 2000; Quinn et al., 1996) chimeras were used to overcome these problems and study roles for *Pax6* during complex tissue–tissue interactions and in tissues that do not form in the mutants. Production of chimeras allows fine-scale analysis of autonomy and non-autonomy of gene function at the single cell level (Rossant and Spence, 1998; West, 1999) and is especially useful to study tissues where promoters that efficiently target expres-

* Corresponding author. Fax: +44-1224-555719.

E-mail address: m.collinson@abdn.ac.uk (J.M. Collinson).

[1] Current address: Department of Biomedical Sciences, Institute of Medical Sciences, University of Aberdeen, Foresterhill, Aberdeen AB25 2ZD, Scotland, UK.

0012-1606/03/$ – see front matter © 2003 Elsevier Science (USA). All rights reserved.
doi:10.1016/S0012-1606(02)00095-7

sion of Cre recombinase have not been identified. By making *Pax6*$^{+/+}$ ↔ *Pax6*$^{-/-}$ chimeras that were a mixture of wild-type and *Pax6*$^{-/-}$ cells, Quinn et al. (1996) showed that in chimeras that were composed of less than ~50% *Pax6*$^{-/-}$ cells ("low-percentage chimeras"), invaginated nasal epithelia were formed and eyes developed that had a lens, two-layered retina (an inner layer that is the prospective neural retina and outer layer that will become the RPE), and cornea. Analysis of the distribution of *Pax6*$^{-/-}$ cells in such chimeras at E12.5 showed that mutant cells could not contribute to the nasal epithelium or the lens. Mutant cells were present at extremely low frequency in the neural retina and could contribute to the outer layer of the optic cup, the presumptive RPE, but did not form pigment.

Collinson et al. (2000) showed that the near-exclusion of mutant cells from the future lens and retina was manifest at E9.5, and that *Pax6* is required for maintenance of lens competence and for the adhesion of the optic vesicle to the prospective lens placode. The study did not address whether there is an autonomous requirement for *Pax6* at or before nasal placode formation. Several other questions relating to the fate of mutant cells during development remained, as follows: (1) Whether *Pax6* is required during differentiation of the corneal epithelium; (2) Whether the mutant cells that were present in the neural retina of E12.5 *Pax6*$^{+/+}$ ↔ *Pax6*$^{-/-}$ chimeras would subsequently be eliminated, or whether they could differentiate; (3) Whether the failure of *Pax6*$^{-/-}$ cells to produce pigment in the chimeric RPE is a developmental block, or merely a delay?

In the present study, analyses of the distribution of *Pax6*$^{-/-}$ cells in series of *Pax6*$^{+/+}$ ↔ *Pax6*$^{-/-}$ chimeras at E9.5, E10.5, E14.5, and E16.5 were performed to address these outstanding issues, which have important implications for our understanding of the common roles of Pax6 in genetic networks controlling development.

Materials and methods

Mouse stocks and production of chimeras

Mouse stocks, their maintenance, and the production of chimeric embryos by aggregation have been described previously (Quinn et al., 1996). Two null mutations of *Pax6* were used, *Pax6*^{Sey} and *Pax6*$^{Sey\text{-}Neu}$ (Hill et al., 1991). Embryos were obtained from a cross between pigmented (*C*/*C*) heterozygous *Pax6*$^{Sey/+}$ males, homozygous for a reiterated silent β-globin transgene marker *TgN*(*Hbb-b1*)*83Clo* (henceforth referred to as *Tg*) (Lo, 1986; Lo et al., 1987), and the glucose phosphate isomerase 1-B, *Gpi1*^{b} allele (*Pax6*$^{Sey/+}$; *C*/*C*; *Tg*$^{+}$/*Tg*$^{+}$; *Gpi1*$^{b/b}$), and superovulated, pigmented, *Gpi1*$^{b/b}$ *Pax6*$^{Sey\text{-}Neu/+}$ females which did not carry the transgene (*Pax6*$^{Sey\text{-}Neu/+}$; *C*/*C*; *Gpi1*$^{b/b}$). Eight-cell embryos were flushed from the reproductive tract at E2.5 and aggregated with eight-cell embryos from an albino, *Gpi1*$^{a/a}$ *Pax6*$^{+/+}$ wild-type cross (BALB/c × A/J)F2 (*Pax6*$^{+/+}$; *c*/*c*; *Gpi1*$^{a/a}$), not carrying the *Tg* transgene. After overnight culture, chimeric embryos were transferred into the uteri of pseudopregnant "CF1" (West and Flockhart, 1994) female mice on day 2.5 of pseudopregnancy, this being taken as E2.5.

Chimeric embryos were dissected into cold phosphate-buffered saline (PBS) and staged according to criteria of forelimb development (Wanek et al., 1989). The head was removed and fixed in 4% (w/v) paraformaldehyde (PFA) in PBS overnight at 4°C, before processing to wax. Tail tissue was removed for PCR genotyping, as described previously (Collinson et al., 2000). The use of two mutant alleles of *Pax6* allowed homozygous mutant chimeras (*Pax6*$^{Sey/Sey\text{-}Neu}$ ↔ *Pax6*$^{+/+}$) to be distinguished from heterozygous chimeras (*Pax6*$^{+/+}$ ↔ *Pax6*$^{Sey/+}$ and *Pax6*$^{+/+}$ ↔ *Pax6*$^{Sey\text{-}Neu/+}$) by PCR.

Tissues from the limbs and trunk were taken for GPI1 analysis, giving a global value of the percentage of cells derived from each aggregated eight-cell embryo in the chimera. For all aggregations, the eight-cell embryo derived from the "wild-type" mating was *Gpi1*$^{a/a}$, and the eight-cell embryo derived from the *Pax6*$^{+/Sey\text{-}Neu}$ × *Pax6*$^{Sey/+}$ mating was *Gpi1*$^{b/b}$. The percentage contribution of GPI1-B was measured by quantitative colorimetric electrophoresis (West and Flockhart, 1994) for all resulting chimeras—those with higher %GPI1-B are primarily composed of cells derived from the small eye mating, and vice versa.

Histological analysis of the distribution of cells from the *Pax6*$^{Sey\text{-}Neu/+}$ × *Pax6*$^{Sey/+}$ embryo was performed by DNA in situ hybridisation on 7-μm sections using digoxigenin-labelled β-globin probe to detect the reiterated *Tg* transgene (Keighren and West, 1993). After in situ hybridisation, the percentage of transgene-positive (*Tg*$^{+}$) cells in various tissues of the eye was calculated by counting the number of *Tg*$^{+}$ and *Tg*$^{-}$ cells.

Primary estimates of %hybridisation-positive cells were corrected as follows on a tissue-by-tissue basis to allow for failure to detect the signal in some *Tg*$^{+}$ cells, due to sectioning through the nucleus. The apparent percentage of hybridisation-positive nuclei in each tissue of (*Pax6*$^{Sey\text{-}Neu/+}$, *Tg*$^{-/-}$) × (*Pax6*$^{Sey/+}$, *Tg*$^{+/+}$) embryos (nonchimeric, 100% *Tg*$^{+/-}$) was counted, and these percentages were used as correction factors when counting the hybridisation-positive cells in the same tissues in chimeras. Unless stated otherwise, numerical results are summarised as mean ± standard error of the mean (SEM). Statistical analysis of count data was performed using *Statview* Statistical Software (Abacus Concepts Inc., CA).

In situ hybridisation for Pax6 and Trp2 expression

Digoxygenin-labelled riboprobes were transcribed from *Pax6* (Grindley et al., 1995) and *Trp2* partial cDNAs using the DIG RNA-labelling kit (SP6/T7) (Roche Diagnostics Ltd., Lewes, UK). The *Trp2* clone was a gift from Dr I. Jackson, MRC Human Genetic Unit, Edinburgh. In situ hybridisation was performed on 7-μm semiserial sections

(Carić et al., 1997). Adjacent sections were hybridised for visualisation of the β-globin transgene as described above. Sections were lightly counterstained with hematoxylin and examined using bright-field microscopy.

Immunohistochemical detection of Pax6

Embryos were fixed in 4% w/v paraformaldehyde, dehydrated, and embedded in paraffin wax. Sections measuring 7 μm were dewaxed and rehydrated, then boiled in 0.01 M citrate buffer, pH 6 for 20 min. After 20 min cooling, slides were rinsed with 50 mM TBS before blocking for 30 min (blocking buffer: 20% normal rabbit serum in TBS). Monoclonal Pax6 antibody from the Developmental Studies Hybridoma Bank was diluted 1:50 in blocking buffer, and sections were incubated in the primary antibody solution for 1 h at room temperature. After four 5-min washes in TBS, secondary antibody (biotin-labelled rabbit anti-mouse (DAKO UK Ltd.) diluted 1:200 in blocking buffer) was added to sections for 30 min at room temperature; then sections were rinsed in TBS four times for 5 min. The avidin/biotin ABC solution (DAKO UK Ltd.) was added to sections, followed by three 5-min washes in TBS. The sections were then stained with diaminobenzidine (Sigma, UK) for 25 min, rinsed in water, dehydrated, and mounted.

Results

Pax6 is required cell-autonomously for development of all layers of the cornea

Immunostaining was performed on sections of paraffin-embedded eye sections at E16.5. Strong expression of Pax6 occurred in the lens and corneal epithelia, and in all layers of the retina, but only very weak labelling was seen in the neural crest derived mesenchymal cells of the corneal stroma and iridocorneal angle (Fig. 1). The pattern of staining was identical to that described recently by Baulmann et al. (2002). Using both immunohistochemistry and X-Gal analysis of the $Pax6^{LacZ}$ mouse, Baulmann et al. found weak Pax6 labelling at E19 in mesenchymal cell nuclei around the iridocorneal angle in the corneal stroma and endothelium, iris stroma, and prospective trabecular meshwork.

To investigate whether Pax6 might have autonomous roles during development of the cornea, 22 E16.5 chimeras were produced. Genotypic analysis showed that 6 chimeras were of the $Pax6^{+/+} \leftrightarrow Pax6^{Sey/Sey\text{-}Neu}$ combination (i.e., a mixture of Tg^{-} $Pax6^{+/+}$ and Tg^{+} $Pax6^{Sey/Sey\text{-}Neu}$ cells—henceforth termed $Pax6^{+/+} \leftrightarrow Pax6^{-/-}$) and 10 were either $Pax6^{+/+} \leftrightarrow Pax6^{Sey\text{-}Neu/+}$ or $Pax6^{+/+} \leftrightarrow Pax6^{Sey/+}$. Six were $Pax6^{+/+} \leftrightarrow Pax6^{+/+}$ "control" chimeras composed of Tg^{+} $Pax6^{+/+}$ and Tg^{-} $Pax6^{+/+}$ cells. As described under Materials and methods, the ratio of GPI1-A and GPI1-B allozymes in the trunk of each embryo was determined by quantitative electrophoresis: %GPI1-B was taken as a

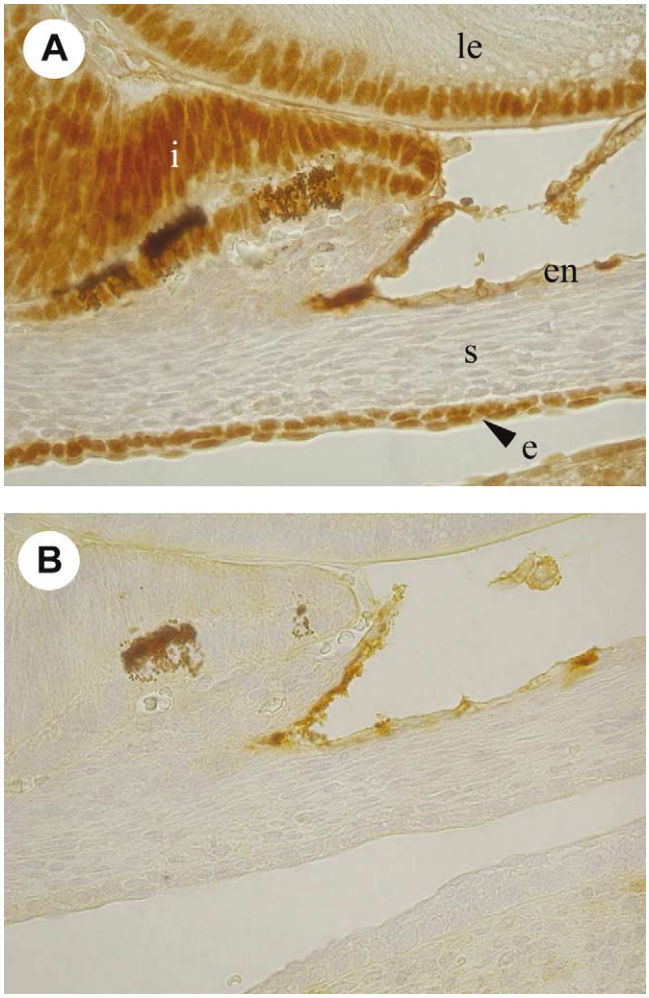

Fig. 1. Expression of Pax6 in the E16.5 eye. (A) Immunohistochemical staining of a $Pax6^{+/+} \leftrightarrow Pax6^{+/+}$ control chimera showing strong staining in the lens and corneal epithelia, the neural retina and distal RPE, and both epithelial layers of the iris. Weak staining is detected in the iris stroma, and cells of the corneal stroma. A negative (no primary antibody) control of an adjacent section (B), stained simultaneously with (A), shows nonspecific staining at the apical surface of the endothelium only, and no nuclear staining in any tissue. Key: le, lens; e, corneal epithelium; s, corneal stroma; en, corneal endotheium; i, iris/ciliary body.

global estimate of the percentage of cells derived from the $Pax6^{Sey\text{-}Neu/+} \times Pax6^{Sey/+}$ eight-cell embryo that was present in the E16.5 chimera. The distribution of these cells in the cornea was identified histologically by DNA in situ hybridisation on wax sections using a digoxigenin-labelled probe which recognised the β-globin transgene *Tg* carried homozygously by the male $Pax6^{Sey/+}$ stud mice. Only "low-percentage" chimeras with <55% mutant cells were used for the analysis, since those with higher proportions of mutant cells lacked lenses and properly differentiated retinas, hence making unequivocal identification of the cornea impossible.

The contribution of Tg^{+}, $Pax6^{-/-}$ cells to the corneal epithelium (Ep), endothelium (En), and stroma (S) of $Pax6^{+/+} \leftrightarrow Pax6^{-/-}$ chimeras was compared to the distribution of Tg^{+} wild-type cells in control chimeras. For all

Table 1
Contribution of cells to different layers of the E16.5 cornea

Eye	B	cornEp%	Ep	Ep/B	cornS%	S	S/B	cornEn%	En	En/B
(i) Control chimeras										
MC268L	41.67	77/802 = 9.601	14.402	0.346	182/2153 = 8.453	12.680	0.304	64/292 = 21.917	28.790	0.691
MC268R	41.67	160/1224 = 13.072	19.608	0.471	465/2828 = 16.443	24.664	0.592	66/312 = 21.150	27.780	0.667
MC232L	48.67	300/1090 = 27.523	41.284	0.848	759/3017 = 25.157	37.736	0.775	101/349 = 28.940	38.010	0.781
MC232R	48.67	241/955 = 25.236	37.853	0.778	611/2587 = 23.618	35.427	0.728	276/581 = 47.504	63.930	1.314
MC228L	31.01	69/676 = 10.207	15.311	0.494	137/1398 = 9.800	14.700	0.474	106/432 = 24.537	33.030	1.065
MC228R	31.01	86/908 = 9.471	14.207	0.458	208/2422 = 8.588	12.882	0.415	116/481 = 24.116	32.450	1.047
MC328L	12.00	17/470 = 3.617	5.426	0.452	39/1003 = 3.888	5.833	0.486	7/196 = 3.571	4.805	0.400
MC328R	12.00	13/381 = 3.412	5.188	0.432	37/1030 = 3.592	5.388	0.449	20/581 = 3.442	4.633	0.386
MC310L	50.00	84/275 = 30.545	45.818	0.916	345/948 = 35.865	53.798	1.076	251/529 = 47.448	63.840	1.277
MC310R	50.00	89/384 = 23.177	34.766	0.695	262/1142 = 23.555	35.333	0.707	262/536 = 48.881	65.780	1.316
Mean				0.589			0.601			0.894
SEM				0.064			0.071			0.113
(ii) Homozygous mutant chimeras										
A/M5L	21.83	2/1003 = 0.181	0.271	0.012	28/2147 = 1.304	1.946	0.089	8/402 = 1.990	2.678	0.123
A/M5R	21.83	1/1063 = 0.094	0.141	0.006	63/2517 = 2.503	3.754	0.172	9/417 = 2.158	2.904	0.133
A/M11L	39.80	2/757 = 0.264	0.396	0.010	110/1388 = 7.925	11.887	0.299	8/281 = 2.856	3.844	0.097
MC230L	19.33	2/506 = 0.395	0.592	0.031	51/1666 = 3.061	4.592	0.238	5/300 = 1.167	1.571	0.081
MC230R	19.33	0/585 = 0.000	0.000	0.000	27/2228 = 1.212	1.809	0.094	1/449 = 0.223	0.300	0.016
MC272R	33.73	1/621 = 0.161	0.241	0.007	97/1985 = 4.887	7.330	0.217	30/348 = 8.621	11.602	0.343
MC272L	33.73	1/568 = 0.176	0.263	0.008	178/1897 = 9.383	14.005	0.415	29/364 = 7.967	10.722	0.318
MC270L	5.53	0/1900 = 0.000	0.000	0.000	2/4940 = 0.041	0.061	0.011	1/1140 = 0.001	0.001	0.000
Mean				0.009			0.192			0.139
SEM				0.003			0.046			0.044

Note. B = %GPIl-B of chimera; SEM = standard error of the mean. cornEp%, cornS%, cornEn% = number of T_g^+ cells divided by number of cells scored and expressed as a percentage in corneal epithelium, stroma, and endothelium, respectively. Ep, S, En = cornEp%, cornS%, and cornEn%, respectively, multiplied by correction factors described under Materials and methods.

chimeric eyes, the $\%Tg^+$ cells in the three layers of the cornea was calculated separately and divided by the %GPI1-B (B) of the chimera. These data are presented in full in Table 1 and summarised in Fig. 2. The mean Ep/B ratio for $Pax6^{+/+} \leftrightarrow Pax6^{-/-}$ chimeras (0.009 ± 0.003 SEM; $n = 8$ eyes) was significantly lower than Ep/B of $Pax6^{+/+} \leftrightarrow Pax6^{+/+}$ controls (0.589 ± 0.064; $n = 10$; *t*-test: $P < 0.0001$) (Fig. 2A). Hence $Pax6^{-/-}$ cells were severely underrepresented in the corneal epithelium, a tissue in which high levels of Pax6 protein are detected. In comparison to control chimeras, $Pax6^{-/-}$, Tg^+ cells were also underrepresented in the corneal stroma and endothelium, albeit less dramatically. The mean S/B ratio for the stroma of $Pax6^{+/+} \leftrightarrow Pax6^{-/-}$ chimeras was 0.192 ± 0.046, $n = 8$, which is significantly less than the mean S/B ratio for $Pax6^{+/+} \leftrightarrow Pax6^{+/+}$ chimeras (0.601 ± 0.071, $n = 10$; *t*-test $P < 0.001$) (Fig. 2B). In the endothelium, the mean En/B ratio for $Pax6^{+/+} \leftrightarrow Pax6^{-/-}$ chimeras was 0.139 ± 0.044, $n = 8$, significantly less than the mean En/B ratio for $Pax6^{+/+} \leftrightarrow Pax6^{+/+}$ chimeras (0.894 ± 0.113, $n = 10$; *t*-test, $P < 0.0001$) (Fig. 2C). Thus, there is an autonomous requirement for functional Pax6 for full and normal contribution of cells to all layers of the cornea. This had not previously been demonstrated. The effect is most pronounced in the tissue with highest levels of *Pax6* expression.

In chimeras studied previously at E9.5 (Collinson et al., 2000), it was found that $Pax6^{-/-}$ cells in $Pax6^{+/+} \leftrightarrow Pax6^{-/-}$ chimeras were eliminated from an area of the facial epithelium wider than the lens placode. This potentially included, at least in part, the anlage fated to become the corneal epithelium. It was therefore possible that the absence of mutant cells from the E16.5 chimeric corneal epithelium was a result of a much earlier elimination at E9.5 and did not represent a specific failure of mutant cells to contribute to differentiating corneal epithelium. The contribution of $Pax6^{-/-}$ cells to the corneal epithelium overlying the invaginating lens in a series of E10.5 $Pax6^{+/+} \leftrightarrow Pax6^{-/-}$ chimeras was therefore investigated. By counting the presence of Tg^+, $Pax6^{-/-}$ cells in the prospective corneal epithelium of each eye at E10.5 (Ep) and dividing by the %GPI1-B for that chimera, it was found that mutant cells had already repopulated the prospective corneal epithelium (Ep/B = 0.676 ± 0.123; $n = 11$). As an approximate comparison, Tg^+ $Pax6^{+/+}$ cells were counted in the prospective corneas of three $Pax6^{+/+} \leftrightarrow Pax6^{+/+}$ E10.5 chimeras, giving a mean Ep/B ratio of 0.921 ± 0.210. Qualitatively, $Pax6^{-/-}$ cells were also present in the corneal epithelium of E12.5 chimeras of Quinn et al. (1996).

It is concluded that $Pax6^{-/-}$ cells are present in significant numbers in the corneal epithelia of E10.5 $Pax6^{+/+} \leftrightarrow$

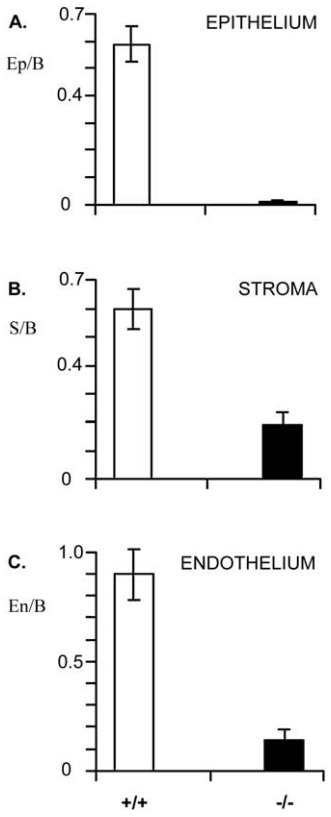

Fig. 2. Underrepresentation of $Pax6^{-/-}$ cells in (A) the E16.5 corneal epithelium, (B) corneal stroma, and (C) corneal endothelium. For each chimeric eye, the percentage of Tg^{+} cells in the corneal epithelium, Ep, stroma, S, and endothelium, En, was divided by global %GPI1-B, B, for that chimera. Mean values ± standard errors are plotted for 10 control $Pax6^{+/+} \leftrightarrow Pax6^{+/+}$ Tg^{+} eyes (white columns) and 8 $Pax6^{+/+} \leftrightarrow Pax6^{-/-}$ Tg^{+} eyes (black columns). Small values of Ep/B, S/B, and En/B indicate that $Pax6^{-/-}$ cells are underrepresented in all layers of the cornea, present in proportions that do not reflect the global composition of the chimera.

$Pax6^{-/-}$ chimeras and are still readily detectable at E12.5. Their absence at E16.5 therefore represents a specific elimination that does not result solely from the proven requirement for Pax6 in the E9.5 facial epithelium. Pax6 is autonomously required for normal contribution to the corneal epithelium between E10.5 and E16.5.

Pax6 is required for normal retinal development

In E16.5 $Pax6^{+/+} \leftrightarrow Pax6^{+/+}$ and $Pax6^{+/+} \leftrightarrow Pax6^{+/-}$ chimeras, $Pax6^{+/+}$ or $Pax6^{+/-}$ cells, respectively, were detected in all layers of the retina, forming clonally related stripes as reported previously (Fig. 3A; Collinson et al., 2001). $Pax6^{-/-}$ Tg^{+} cells were detected at very low frequencies in the retinas of $Pax6^{+/+} \leftrightarrow Pax6^{-/-}$ chimeras, as aggregations of up to 100 cells almost exclusively in the developing ganglion cell layer (Fig. 3B and C). In three retinas small groups of up to 10 $Pax6^{-/-}$ Tg^{+} cells were seen in sections of the undifferentiated inner/outer nuclear layer (Fig. 3D). Stripes of $Pax6^{-/-}$ Tg^{+} cells spanning the thickness of the retina were never observed. The underrepresentation $Pax6^{-/-}$ cells in the E16.5 retina and their abnormal clonal arrangement demonstrate that *Pax6* is required for normal contribution of cells to the retina during development. Because of the very small proportions of $Pax6^{-/-}$ cells in the retinas at this age, it was not possible to determine, by the use of molecular markers, whether the mutant cells were differentiating appropriately for their location.

Absence of Pax6 delays but does not prevent pigmentation of the RPE

In the outer layer of the optic cup (the prospective RPE) of the E16.5 chimeras, $Pax6^{-/-}$ cells, although underrepresented, were present at higher frequency than in the neural retina. In most cases (five of six retinas that were examined serially), some of these mutant cells had produced pigment, showing that *Pax6* is not absolutely required for melanin production in the RPE (Fig. 3E). In comparison with the E12.5 chimeras produced by Quinn et al. (1996), in which mutant cells did not produce pigment, it can now be concluded that absence of Pax6 delays the full differentiation of RPE cells but does not prevent it.

To investigate the molecular basis of pigmentation in the mutant cells, in situ hybridisation was performed on E14.5 chimeric tissues, prior to the appearance of pigment, using probes against *Pax6* and *Trp2*, an early marker of the RPE pigmentation pathway (Fig. 3F–K). In control E14.5 eyes, it was confirmed that *Trp2* expression is confined to the RPE and scattered melanocytes in the extraocular mesenchyme (Fig. 3F), whereas *Pax6* is expressed in all layers of the retina, and the corneal and lens epithelia (Fig. 3G and K). *Trp2* expression was detectable in all $Pax6^{-/-}$ cells in the outer layer (the presumptive RPE) of the bilayered optic cup in E14.5 $Pax6^{+/+} \leftrightarrow Pax6^{-/-}$ chimeras (Fig. 3H, I, and J). This demonstrated that absence of *Pax6* does not preclude the expression of genes in the normal RPE pigmentation pathway.

Early roles for Pax6 during the differentiation of the olfactory epithelium

During normal development, nasal placodes are induced in the facial ectoderm at E9.5, which subsequently involute to form the olfactory epithelia. Grindley et al. (1995) demonstrated that *Pax6* is expressed throughout this process and that nasal development ceases at E9.5 in the mutant mice. They could, however, not distinguish whether this was an autonomous failure of the nasal epithelium or whether it represented a failure of exogenous inductive signals necessary for nasal placode formation.

To address this question, the prospective nasal epithelia of E9.5 $Pax6^{+/+} \leftrightarrow Pax6^{+/+}$, Tg^{+} chimeras and $Pax6^{+/+} \leftrightarrow Pax6^{-/-}$, Tg^{+} chimeras were compared. At E9.5, a broad area of thickened epithelium includes the prospective nasal placode, but the placode itself is not yet a discrete recognisable structure (J.M.C., personal observation). The proportion of Tg^{+} cells in the nasal epithelium (expressed as a

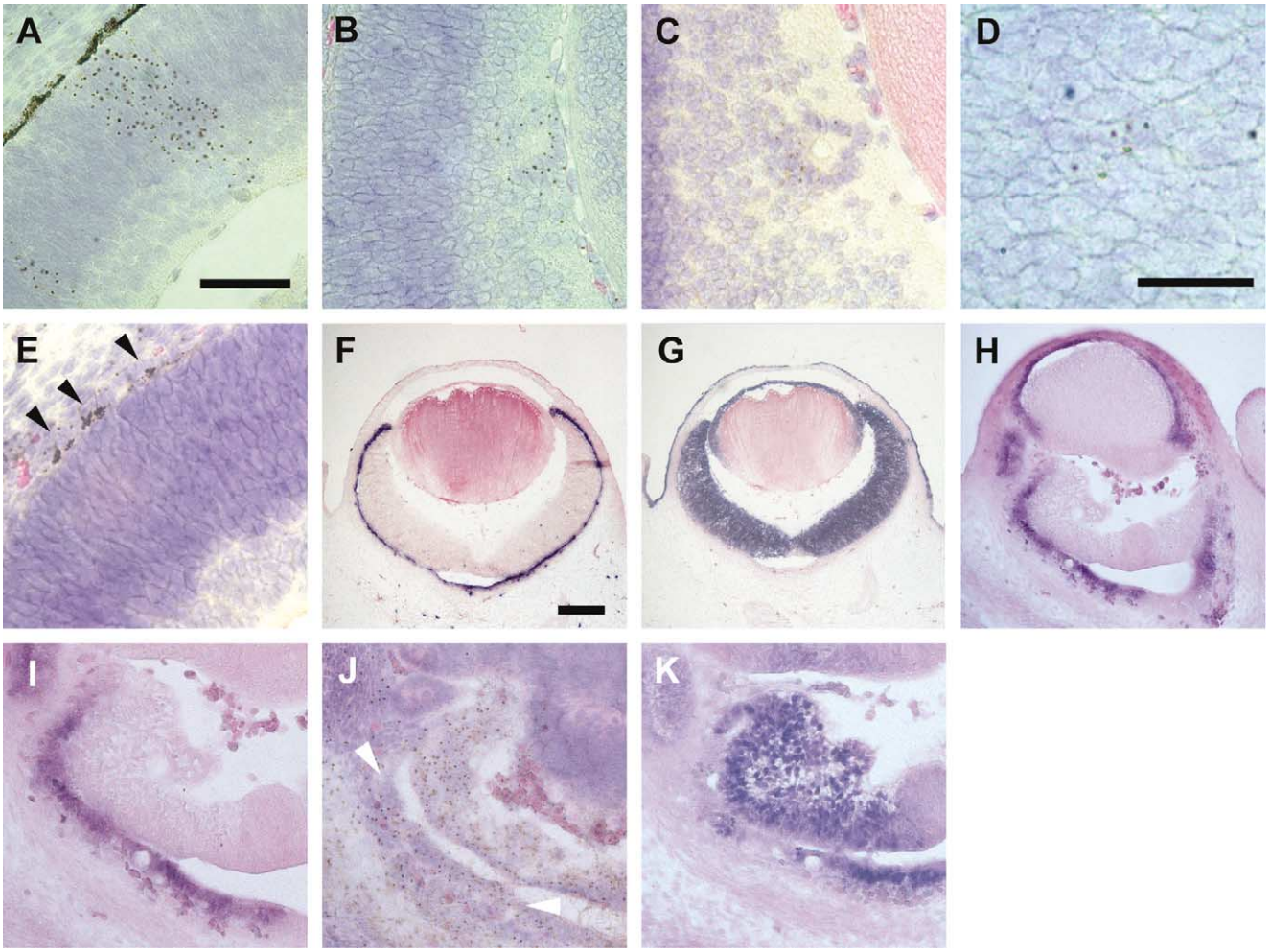

Fig. 3. Contribution of *Pax6*$^{-/-}$ cells and expression of genetic markers in the chimeric retina at E16.5 (A–E) and E14.5 (F–K). (A) Normal distribution of *Tg*$^{+}$ *Pax6*$^{+/+}$ cells revealed by the presence of brown dots in nuclei in an E16.5 control chimera, after DNA–DNA in situ hybridisation using a DIG-labelled β-globin probe against the *Tg* transgene. Stripes of clonally related cells span all layers of the neural retina. (B, C) Abnormal clumps of *Tg*$^{+}$ *Pax6*$^{-/-}$ cells in the ganglion cell layer of a chimera. Stripes of cells equivalent to that seen in (A) were never observed. (D) A small group of *Pax6*$^{-/-}$ cells in the undifferentiated nuclear cell layer of a *Pax6*$^{+/+}$ ↔ *Pax6*$^{-/-}$ chimera. (E) Pigmented *Pax6*$^{-/-}$ cells (arrowheads) in the RPE of a *Pax6*$^{+/+}$ ↔ *Pax6*$^{-/-}$ chimera. (F) In situ hybridisation showing *Trp2* expression in the prospective RPE of a *Pax6*$^{+/+}$ ↔ *Pax6*$^{+/+}$ chimeric control E14.5 eye. (G) *Pax6* expression in an adjacent section to (F). (H) *Trp2* expression in the retina of a E14.5 *Pax6*$^{+/+}$ ↔ *Pax6*$^{-/-}$ chimera composed of 83% *Pax6*$^{-/-}$ cells. Unlike low percentage chimeras, no lens is present and the retina is abnormally folded; in this section, the convoluted retina is composed of two bilayered loops of tissue with a thick inner layer (presumptive neural retina) and a thinner outer layer that expresses *Trp2* (presumptive RPE). (I) Enlarged section of H, showing *Trp2* expression in prospective RPE of lower loop. (J) In situ hybridisation for the β-globin transgene to reveal the location of *Pax6*$^{-/-}$ cells on an adjacent section to (I) shows that the lower loop of retina in H is largely composed of mutant cells. The area of prospective RPE between the arrowheads, shown in (I) to be *Trp2*-positive, is composed almost exclusively of mutant cells. The upper loop of retinal tissue (top right) is exclusively composed of wild-type cells. Both mutant and wild-type RPE cells in the chimeras therefore express *Trp2*. (K) *Pax6* expression in an adjacent section to (I) and (J) shows that the mutant *Pax6* mRNA is present *Pax6*$^{-/-}$ RPE, but the levels of expression are patchy. Scale bars represent (A) 40 μm; (D) 10 μm; (F) 100 μm.

percentage, N) was counted for each E9.5 chimera produced in a previous study (Collinson et al., 2000) and divided by the contribution of *Tg*$^{+}$ cells to the ectoderm round the dorsal side of the head that does not express *Pax6* (H). The ratio N/H was calculated as an indication of any underrepresentation of *Tg*$^{+}$ cells in the prospective preplacodal nasal epithelium at E9.5 compared to the nonspecialised head ectoderm.

For *Pax6*$^{+/+}$ ↔ *Pax6*$^{+/+}$ chimeras N/H = 1.032 ± 0.080, $n = 8$, confirming that *Pax6*$^{+/+}$, *Tg*$^{+}$ cells are equally distributed between the nasal epithelium and other regions of the head. In contrast, for *Pax6*$^{+/+}$ ↔ *Pax6*$^{-/-}$ chimeras, N/H = 0.358 ± 0.052, $n = 13$. These values are very significantly different (t-test: $P < 0.00001$). This demonstrates that there is an autonomous requirement for *Pax6* in the preplacodal nasal epithelium, such that homozygous mutant cells cannot fully contribute. The elimination of mutant cells is not absolute, however, and not as complete as is seen in the prospective lens placode at this stage: calculation of the %*Tg*$^{+}$ cells in the prospective lens placode of low percentage *Pax6*$^{+/+}$ ↔ *Pax6*$^{-/-}$ *Tg*$^{+}$ chimeras (L) (data in Collinson et al., 2000) gave mean L/H = 0.187

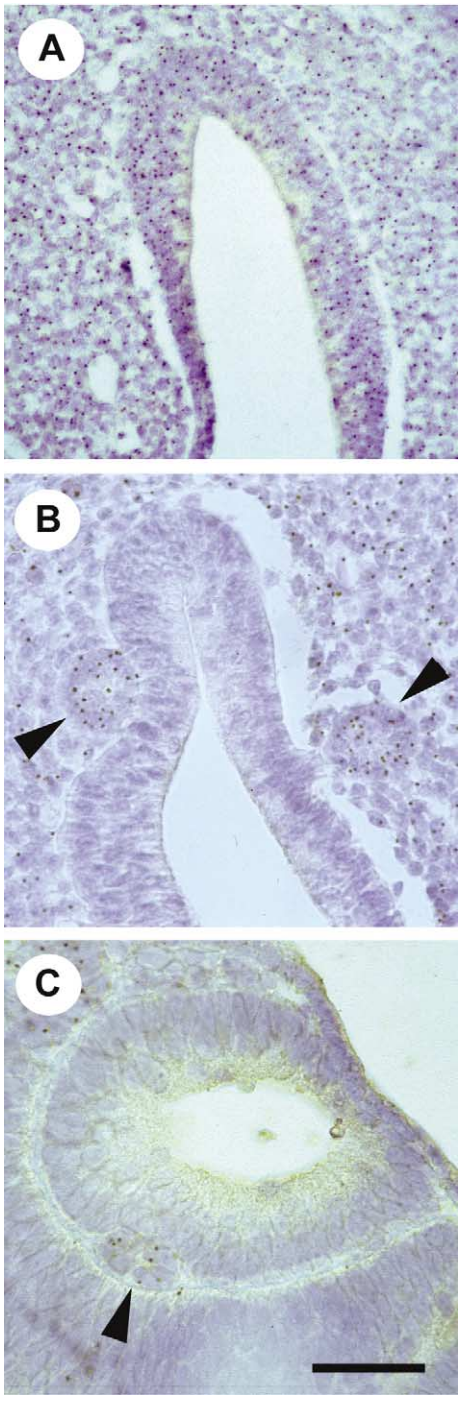

Fig. 4. Physical elimination of $Pax6^{-/-}$ cells from the invaginating nasal epithelium and lens. (A) Nasal epithelium of an E10.5 control chimera, after DNA–DNA in situ hybridisation to detect the *Tg* transgene. Tg^{+} $Pax6^{+/+}$ cells (brown dots in nuclei) are distributed randomly throughout the olfactory epithelium. (B) Distribution of Tg^{+} $Pax6^{-/-}$ cells in the olfactory epithelium of an equivalent E10.5 $Pax6^{+/+} \leftrightarrow Pax6^{-/-}$ chimera. Mutant cells are not present in the normal invaginating structure, but are confined to vesicle-like outgrowths (arrowheads). The exogenous structures are partly contiguous with the olfactory epithelium (a stalk of tissue can be seen to connect the right-hand ectopic bud to the olfactory epithelium). (C) The lens vesicle of an E10.5 $Pax6^{+/+} \leftrightarrow Pax6^{-/-}$ chimera. The lens is entirely wild-type apart from a small bleb of $Pax6^{-/-}$ cells (arrowhead) projecting from the posterior edge. Note that this bleb of cells is contained within the basement membrane of the lens vesicle. Scale bar represents 20 μm.

$\pm$ 0.070, $n = 8$. We suggest that there is a decrease in the rate of proliferation, or an increase in apoptosis, or perhaps movement of mutant cells out of the *Pax6*-expressing lens and nasal regions, but that these processes are more pronounced, or start earlier, in the lens. A new series of experiments will be needed to examine these possibilities.

Exclusion of $Pax6^{-/-}$ cells from invaginating lens and nasal placodes

To investigate the fate of the small proportion of mutant cells that were retained in the prospective nasal epithelium at E9.5, the nasal epithelia of a series of 14 control and 10 $Pax6^{+/+} \leftrightarrow Pax6^{-/-}$, E10.5 chimeras were examined. In $Pax6^{+/+} \leftrightarrow Pax6^{+/+}$, Tg^{+} chimeras, Tg^{+} cells were distributed randomly throughout the invaginating nasal placode as expected (Fig. 4A). In contrast, the invaginating epithelium of $Pax6^{+/+} \leftrightarrow Pax6^{-/-}$ chimeras was composed almost entirely of wild-type cells. In most cases, ectopic buds composed of entirely $Pax6^{-/-}$ cells were detected, projecting into the mesenchyme but contiguous with the nasal epithelium (Fig. 4B). Similar ectopic buds were never seen in control chimeras. These ectopic buds were interpreted as representing mutant cells that were being physically excluded from the differentiating nasal epithelium. That no such structures were seen at E12.5 by Quinn et al. (1996) suggests that they are short-lived and may be eliminated by apoptosis. Hence there are at least two stages (preplacodal and during invagination of the placode) at which Pax6 is required for normal development and differentiation of the nasal epithelium.

Collinson et al. (2000) demonstrated that homozygous mutant cells were almost eliminated in a region of facial epithelium that was wider than, but included, the prospective lens placode. The present study shows that the region of near-exclusion also includes the prospective nasal placode, which may fall within the same domain of facial *Pax6* expression (Grindley et al., 1995). To investigate the fate of $Pax6^{-/-}$ cells that are retained in the prospective lens placode at E9.5, the lenses of the E10.5 chimeras were studied. In line with the more complete exclusion of mutant cells from the E9.5 lens than from the nasal region, the invaginating lenses of E10.5 chimeras were almost exclusively wild-type. In two chimeras, a small rosette of mutant cells was found adjacent to the posterior of the lens (Fig. 4C). Because this was never seen in control chimeras or wild-type embryos, we postulate that these mutant rosettes may also be the result of physical exclusion from the invaginating placode.

Discussion

Roles of Pax6 in the cornea

Chimeric studies have now demonstrated autonomous roles for Pax6 in all eye tissues where it is expressed, at

Table 2
Summary of roles of Pax6 in the eye and nasal epithelium at different developmental stages, determined from studies of chimeras

Stage	Eye tissues studied	Roles of Pax6	References
E9.5	Optic vesicle, lens placode, nasal epithelium	Maintenance of placodal competence. Adhesion of optic vesicle to lens placode. Proximodistal specification of optic vesicle.	Collinson et al., 2000; this study.
E10.5	Lens, nasal epithelium, corneal anlage	Required for contribution to invaginating lens and nasal placodes. Dosage effects responsible for failure of heterozygote cells to contribute fully to lens placode.	Collinson et al., 2001; this study.
E12.5	Lens, optic cup, cornea, nasal epithelium	Controls cell-surface properties of neural retina. Required for contribution to lens and nasal epithelia. Required for normal pigmentation of RPE.	Quinn et al., 1996; Collinson et al., 2001; this study.
E14.5	Lens, retina	Not required for molecular specification of RPE.	This study.
E16.5	Lens, cornea, retina, iris	Correct Pax6 dosage required for lens to organise anterior segment. Required for development of all layers of cornea. Retinal cell development. Normal pigmentation of RPE.	Collinson et al., 2001; this study.

several developmental stages, while suggesting that Pax6 dosage in the lens is most critical for normal eye development (Collinson et al., 2000, 2001; Quinn et al., 1996; this study). The chimeric studies are summarised in Table 2.

Multiple abnormalities in the corneas of heterozygous $Pax6^{+/LacZ}$ and $Pax6^{+/Sey\text{-}Neu}$ mice have been reported (Baulmann et al., 2002; Ramaesh et al., 2003). From E18.5 the corneal epithelium is thinner than wild-type, and the stroma is hypercellular, with an irregular laminar arrangement and other defects. These phenotypes become more severe with age and are hypothesised to reflect failure of corneal maintenance in response to environmental injury. In a previous study no underrepresentation of $Pax6^{+/-}$ cells was found in the corneas of E16.5 $Pax6^{+/+} \leftrightarrow Pax6^{+/-}$ chimeras (Collinson et al., 2001), suggesting that the defects in the *heterozygous* cornea are not a result of cell-autonomous failure of primary development.

In this study, it was shown that *homozygous* $Pax6^{-/-}$ cells do not contribute to the corneal epithelium of E16.5 $Pax6^{+/+} \leftrightarrow Pax6^{-/-}$ chimeras, even though they were present at E10.5 and E12.5. Functional Pax6 is therefore an absolute requirement of normal participation in the early development of the corneal epithelium, a tissue in which *Pax6* expression levels are high.

More surprisingly, functional *Pax6* was also required for full participation in the development of the corneal stroma and endothelium. *Pax6* expression in these neural crest derived tissues has recently been detected in mid-late fetal stages (using two different antibodies and *Lac*Z staining) and is very much weaker that that seen in other eye tissues (Fig. 1; Baulmann et al., 2002). However, *Pax6* is expressed broadly in the forebrain from E8 and the forebrain-derived neural crest cells that populate the periocular mesenchyme (Trainor and Tam, 1995) may retain *Pax6* expression at earlier stages. Defects in migration of cranial neural crest cells in $Pax6^{-/-}$ embryos have been demonstrated, although the evidence suggested that these were a nonautonomous consequence of the failure of signaling from the frontonasal ectoderm (Matsuo et al., 1993; Osumi-Yamashita et al., 1997). Our data suggest that these failures are at least in part cell-autonomous and are the first proven autonomous roles for Pax6 in a neural crest-derived tissue.

Roles of Pax6 in the retina

We found that $Pax6^{-/-}$ cells could, albeit in small numbers, contribute to the ganglion cell layer at E16.5 and were also detectable in the nuclear layers. Mutant cells in the ganglion layer appeared abnormal, forming tight clusters or having a vesicular appearance, and it is perhaps unlikely that they were differentiating correctly. The contribution to the ganglion cell layer is unexpected in light of a complementary study in which *Pax6* was inactivated in the distal retina during early embryogenesis (Marquardt et al., 2001). In that study, $Pax6^{-/-}$ cells differentiated as amacrine cells but could not form any other retinal cell type. The most likely explanation for the discrepancy between the two studies is that in the Marquardt et al. Cre-*lox* system, *Pax6* was not inactivated until E10.5, whereas cells in our chimeras have never had functional Pax6. Generation of retinal cells occurs in chronological sequence, with ganglion and horizontal cells appearing first, followed by amacrine and other cell types (Young, 1985). Given the stepwise and progressive nature of retinal development from early embryogenesis, it is perhaps possible that the $Pax6^{-/-}$ cells in our chimeras develop cell-surface characteristics that are different from those cells that lose their *Pax6* expression at E10.5. The cells in our study may represent a more immature stage of retinal development, lagging any normally differentiating cell type but most closely resembling the earliest born ganglion cells. Alternatively, because displaced amacrine cells are a normal constituent of the mouse ganglion cell layer (Jeon et al., 1998), it is equally possible that mutant cells seen in the chimeric retinas may be ama-

crine-like cells that are stranded in an ectopic retinal location.

In the RPE, the presence of a small proportion of pigmented Pax6$^{-/-}$ cells showed that absence of functional Pax6 delays differentiation but does not always prevent it. Because both the alleles of *Pax6* used in this study, *Pax6^{Sey}* and *Pax6$^{Sey\text{-}Neu}$*, are point mutations, the possibility was considered that the pigmented cells in the RPE were the result of rare somatic back-mutations that restored functionality to one of the alleles. This hypothesis cannot be formally eliminated; however, we believe it to be extremely unlikely. *Pax6$^{-/-}$* cells (*Tg^{+}*) are heavily underrepresented in the RPE, so back-mutation would have to be very common to produce pigmented cells in five of six serially examined RPEs. This frequency would be greater than that reported for the dilute mutation, which is caused by a viral insertion and produced only 1 somatic and 10 germ-line reversions among more than a million mice (Seperack et al., 1988). It would be even greater than the reversion rate of the *laacZ* transgene, which was designed as an unstable transgene for use as a lineage marker and reverted by random intragenic recombination to form 128 *lac*Z clones in the brains of 1200 postnatal mice (Mathis et al., 1997). Also, if *Pax6^{Sey}* or *Pax6$^{Sey\text{-}Neu}$* back-mutated to wild-type *Pax6^{+}* at such a high frequency to produce revertant clones in five of six RPEs, we would expect at least occasional instances of back-mutation in the neural retina of *Pax6$^{+/+}$* ↔ *Pax6$^{-/-}$* chimeras to produce thin clonal stripes of *Tg^{+}* cells contributing to and differentiating appropriately within one or more layers of this epithelium. Such an event has never been observed nor have we ever seen unexpected contributions of homozygous mutant *Tg^{+}* cells to tissues such as the lens or corneal epithelium that might be explained by back-mutation during early embryogenesis. Furthermore, it was shown that *Pax6$^{-/-}$* cells in the presumptive RPE of E14.5 *Pax6$^{+/+}$* ↔ *Pax6$^{-/-}$* chimeras express the early pigmentation marker, *Trp2*, showing that the differentiation pathway is underway in too many cells to be explained by back-mutation.

Roles for Pax6 in the prospective lens and nasal epithelia

Collinson et al. (2000) showed that Pax6 was required in the preplacodal lens epithelium, and Ashery-Padan et al. (2000) demonstrated a requirement at lens placode induction. The present study has extended these results to show that functional *Pax6* is required autonomously for full contribution of cells to an area of the facial epithelium that includes the prospective nasal placode and is then absolutely required during the early stages of differentiation of the invaginating olfactory epithelium and lens placode. This pattern of multiple roles during the differentiation of a single tissue is characteristic of *Pax6* (Cvekl and Piatigorsky, 1996) and is qualitatively identical in the lens and nasal placodes.

The developmental process of lens induction is perhaps best understood in *Xenopus*, where a "lens-competent" anterior region of early epithelium becomes progressively biased and then determined to form the lens by a series of inductive interactions (Grainger et al., 1988; Grainger, 1992). The area of the face that is competent to form a lens is proportionately large, and many of the lens-competent cells will not subsequently participate in lens placode formation. Experiments performed in mouse and chicken suggest that similar processes of progressive induction of a subset of lens-competent cells occur in these species (Barabanov and Fedtsova, 1982; Enwright and Grainger, 1999; Piatigorsky, 1981). The domain of *Pax6* expression in the facial epithelium at E8.5–9 is extensive and, at least in the mouse, appears to overlap both the prospective lens and the nasal placodes (Grindley et al., 1995). In the case of the lens, the domain of *Pax6* expression has been implicated in defining a region of lens-competence (Li et al., 1994), and our previous study (Collinson et al., 2000) provided evidence for this assertion. Hogan et al. (1986) first suggested that a common role for Pax6 in lens and olfactory placodes might underlie their failure in *Pax6$^{-/-}$* mutants. Because the expression domain of *Pax6* at E8.5–E9 may encompass both the prospective lens and the nasal placodes, it would now be tempting to speculate that *Pax6* expression in the face defines a less specific region of "placode-forming competence." The loss of *Pax6$^{-/-}$* cells from the preplacodal or early-placodal nasal epithelium demonstrated in this study is evidence that Pax6 is required for maintaining the tissue-competence that mediates nasal placode formation, and hence, that *Pax6* is indeed required to maintain the "placodal competence" within the facial epithelium.

Segregation of *Pax6* mutant cells from wild-type in chimeras was seen again in this study as it has been in all our previous and current studies in the eye and brain (Collinson et al., 2000, 2001; Pratt et al., 2002; Quinn et al., 1996; Talamillo et al., 2003). This is a predicted consequence of the control of downstream cell-surface molecules by *Pax6* (Duncan et al., 2000; Stoykova et al., 1997). The apparent physical exclusion of mutant cells from both the invaginating nasal and, sometimes, the lens placodes at E10.5 seen in this study argues that *Pax6* may have similar roles in these two structures, possibly via the control of the same cell-surface molecules. More E10.5 chimeric eyes will be needed to confirm this hypothesis. We conceptualise a model in which the common functions for Pax6 in the facial sensory region maintain the competence to form lens and nasal placodes and then control the cell-surface properties that mediate their morphogenesis. The very different fates of the nasal and lens placodes are presumably a consequence of lens and nasal-specific genes that are coexpressed with *Pax6* as a result of the different inductive influences to which they are exposed. This model is consistent with hypothesised ancestral roles for Pax6 as a mediator of sensory organ formation at the anterior of the head.

Acknowledgments

We thank Denis Doogan, Maureen Ross, and Jim Macdonald for specialist assistance and Jean Flockhart and Margaret Keighren for advice and help during the project. This work was supported by Medical Research Council Award No. G9630132 to J.D.W.

References

Ashery-Padan, R., Marquardt, T., Zhou, X., Gruss, P., 2000. Pax6 activity in the lens primordium is required for lens formation and for correct placement of a single retina in the eye. Genes Dev. 14, 2701–2711.

Barabanov, V.M., Fedtsova, N.G., 1982. The distribution of lens differentiation capacity in the head ectoderm of chick embryos. Differentiation 21, 183–190.

Baulmann, D.C., Ohlmann, A., Flügel-Koch, C, Goswami, S., Cvekl, A., Tamm, E.R., 2002. Pax6 heterozygous eyes show defects in chamber angle differentiation that are associated with a wide spectrum of other anterior segment abnormalities. Mech. Dev. 118, 3–17.

Carić, D., Gooday, D., Hill, R.E., McConnell, S.K., Price, D.J., 1997. Determination of the migratory capacity of embryonic cortical cells lacking the transcription factor Pax-6. Development 124, 5087–5096.

Collinson, J.M., Hill, R.E., West, J.D., 2000. Different roles for Pax6 in the optic vesicle and facial epithelia mediate early morphogenesis of the murine eye. Development 127, 945–956.

Collinson, J.M., Quinn, J.C., Buchanan, M.A., Wedden, S.E., Kaufman, M.H., West, J.D., Hill, R.E., 2001. Primary defects in the lens underlie complex anterior segment abnormalities in the Pax6 heterozygous eye. Proc. Natl. Acad. Sci. USA 98, 9688–9693.

Cvekl, A., Piatigorsky, J., 1996. Lens development and crystallin gene expression: many roles for Pax-6. Bioessays 18, 621–630.

Duncan, M.K., Kozmik, Z., Cveklova, K., Piatigorsky, J., Cvekl, A., 2000. Overexpression of PAX6 (5a) in lens fiber cells results in cataract and upregulation of alpha 5 beta 1 integrin expression. J. Cell Sci. 113, 3173–3185.

Enwright, J.F., Grainger, R.M., 1999. An in vitro analysis of murine lens induction in wildtype, and in Pax-6 and Lhx-2 mutant embryos. Dev. Biol. 210, 210.

Grainger, R.M, 1992. Embryonic lens induction: shedding light on vertebrate tissue determination. Trends Genet. 8, 349–355.

Grainger, R.M., Henry, J.J., Henderson, R.A., 1988. Reinvestigation of the role of the optic vesicle in embryonic lens induction. Development 102, 517–526.

Grindley, J.C., Davidson, D.R., Hill, R.E., 1995. The role of Pax-6 in eye and nasal development. Development 121, 1433–1442.

Hill, R.E., Favor, J., Hogan, B.L.M., Ton, C.C.T., Saunders, G.F., Hanson, I.M., Prosser, J., Jordan, T., Hastie, N.D., van Heyningen, V., 1991. Mouse *Small eye* results from mutations in a *paired*-like homeobox-containing gene. Nature 354, 522–525.

Hitchcock, P.F., Macdonald, R.E., VanDeRyt,, J.T., Wilson, S.W., 1996. Antibodies against Pax6 immunostain amacrine and ganglion cells and neuronal progenitors, but not rod precursors, in the normal and regenerating retina of the goldfish. J. Neurobiology 29, 399–413.

Hogan, B.L.M., Horsburgh, G., Cohen, J., Hetherington, C.M., Fisher, G., Lyon, M.F., 1986. *Small eyes* (*Sey*): a homozygous lethal mutation on chromosome 2 which affects the differentiation of both lens and nasal placodes in the mouse. J. Embryol. Exp. Morphol. 97, 95–110.

Jeon, C.-J., Strettoi, E., Masland, R.H., 1998. The major cell populations of the mouse retina. J. Neurosci. 18, 8936–8946.

Keighren, M., West, J.D., 1993. Analysis of cell ploidy in histological sections of mouse tissues by DNA-DNA in situ hybridisation with digoxygenin-labelled probes. Histochem. J. 25, 30–44.

Koroma, B.M., Yang, J.-M., Sundin, O.H., 1998. The Pax-6 homeobox gene is expressed throughout the corneal and conjunctival epithelia. Invest. Ophthalmol. Visual Sci. 38, 108–120.

Li, H.-S., Yang, J.-M., Jacobson, R.D., Pasko, D., Sundin, O., 1994. *Pax-6* is first expressed in a region of ectoderm anterior to the early neural plate: implications for stepwise determination of the lens. Dev. Biol. 162, 181–194.

Lo, C., 1986. Localization of low abundance DNA sequences in tissue sections by in situ hybridization. J. Cell Sci. 81, 143–162.

Lo, C.W., Coulling, M., Kirby, C., 1987. Tracking of mouse cell lineage using microinjected DNA sequences: analysis using genomic Southern blotting and tissue-section in situ hybridizations. Differentiation 35, 37–44.

Marquardt, T., Ashery-Padan, R., Andrejewski, N., Scardigli, R., Guillemot, F., Gruss, P., 2001. Pax6 is required for the multipotent state of retinal progenitor cells. Cell 105, 43–55.

Mathis, L., Bonnerot, C., Puelles, L., Nicolas, J.F., 1997. Retrospective clonal analysis of the cerebellum using genetic *laacZ*/*lacZ* mouse mosaics. Development 124, 4089–4104.

Matsuo, T., Osumiyamashita, N., Noji, S., Ohuchi, H., Koyama, E., Myokai, F., Matsuo, N., Taniguchi, S., Doi, H., Iseki, S., Ninomiya, Y., Fujiwara, M., Watanabe, T., Eto, K., 1993. A mutation in the *Pax-6* gene in rat *small eye* is associated with impaired migration of midbrain crest cells. Nat. Genet. 3, 299–304.

Osumi-Yamashita, N., Kuratani, S., Ninomiya, Y., et al., 1997. Cranial abnormality of homozygous rSey rat is associated with a defect in the migration pathway of midbrain crest cells. Dev. Growth Differ. 39, 53–67.

Piatigorsky, J., 1981. Lens differentiation in vertebrates: a review of cellular and molecular features. Differentiation 19, 134–153.

Pratt, T., Quinn, J.C., Simpson, T.I., West, J.D., Mason, J.O., Price, D.J., 2002. Disruption of early events in thalamocortical tract formation in mice lacking the transcription factors Pax6 or Foxg1. J. Neurosci. 22, 8523–8531.

Quinn, J.C., West, J.D., Hill, R.E., 1996. Multiple functions for Pax6 in mouse eye and nasal development. Genes Dev. 10, 435–446.

Ramaesh, T., Collinson, J.M., Ramaesh, K., Kaufman, M.H., West, J.D., Dhillon, B., 2003. Corneal abnormalities in $Pax6^{+/-}$ (small eye) mice mimic human aniridia-related keratopathy. Invest. Ophthalmol. Visual Sci. in press.

Rossant, J., Spence, A., 1998. Chimeras and mosaics in mouse mutant analysis. Trends Genet. 14, 358–363.

Seperack, P.K., Strobel, M.C., Corrow, D.J., Jenkins, N.A., Copeland, N.G., 1988. Somatic and germ-Line reverse mutation-rates of the retrovirus- induced dilute coat-color mutation of DBA mice. Proc. Natl. Acad. Sci. USA 85, 189–192.

Stoykova, A., Gotz, M., Gruss, P., Price, J., 1997. Pax6-dependent regulation of adhesive patterning, R-cadherin expression and boundary formation in developing forebrain. Development 124, 3765–3777.

Talamillo, A., Quinn, J.C., Collinson, J.M., Carić, D., Price, D.J., West, J.D., Hill, R.E., 2003. *Paxó* regulates regional development and neuronal migration in the cerebral cortex. Dev. Biol. 255, 151–163.

Trainor, P.A., Tam, P.P.L., 1995. Cranial paraxial mesoderm and neural crest cells of the mouse embryo: codistribution in the craniofacial mesenchyme but distinct segregation in branchial arches. Development 121, 2569–2582.

Walther, C., Gruss, P., 1991. *Pax-6*, a murine paired box gene, is expressed in the developing CNS. Development 113, 1435–1449.

Wanek, N., Muneoka, K., Holler-Dinsmore, G., Burton, R., Bryant, S.V., 1989. A staging system for mouse limb development. J. Exp. Zool. 249, 41–49.

West, J.D., 1999. Insights into development and genetics from mouse chimeras. Curr. Top. Dev. Biol. 44, 21–66.

West, J.D., Flockhart, J.H., 1994. Genotypically unbalanced diploid ↔ diploid foetal mouse chimaeras: possible relevance to human confined mosaicism. Genet. Res. 63, 87–99.

Young, R.W., 1985. Cell differentiation in the retina of the mouse. Anat. Rec. 212, 199–205.